Alchemical Analysis of FDA Approved Drugs
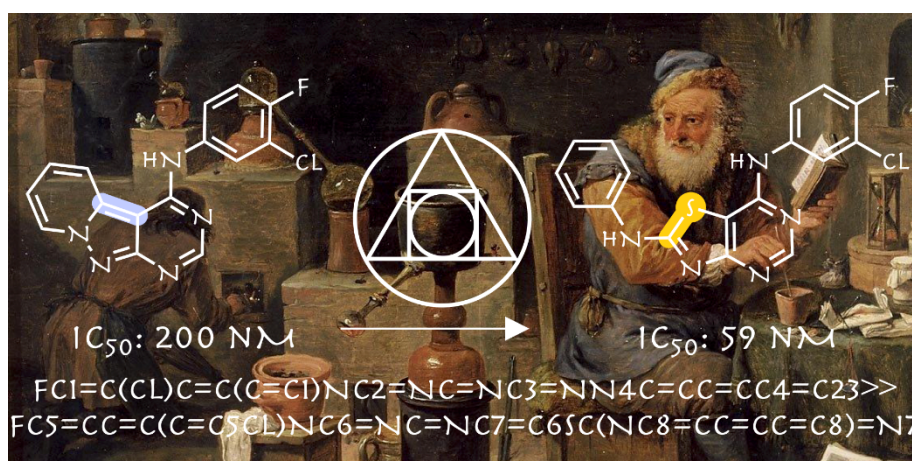
Markus Orsi,[a] Daniel Probst,[b] Philippe Schwaller[b] and Jean-Louis Reymond[a]*

a) Department of Chemistry, Biochemistry and Pharmaceutical Sciences, University of Bern, Freiestrasse 3, 3012 Bern, Switzerland, b)Ecole Polytechnique Fédérale de Lausanne, 1015 Lausanne, Switzerland

e-mail: jean-louis.reymond@unibe.ch

Abstract

Chemical space maps help visualize similarities within molecular sets. However, there are many different molecular similarity measures resulting in a confusing number of possible comparisons. To overcome this limitation, we exploit the fact that tools designed for reaction informatics also work for alchemical processes that do not obey Lavoisier's principle, such as the transmutation of lead into gold. We start by using the differential reaction fingerprint (DRFP) to create tree-maps (TMAPs) representing the chemical space of pairs of drugs selected as being similar according to various molecular fingerprints. We then use the Transformer-based RXNMapper model to understand structural relationships between drugs, and its confidence score to distinguish between pairs related by chemically feasible transformations and pairs related by alchemical transmutations. This analysis reveals a diversity of structural similarity relationships that are otherwise difficult to analyze simultaneously. We exemplify this approach by visualizing FDA-approved drugs, EGFR inhibitors, and polymyxin B analogs.

Introduction

Mapping molecular databases in a chemical space where distances represent similarities between molecules helps to understand their structural similarities and identify relationships that can provide critical insights for drug development and related fields.[1–15] However, molecular similarity can be computed in multiple ways,[16,17] typically using various molecular fingerprints,[18] resulting in a confusing multiplicity of possible chemical space representations.[19,20]

To overcome this limitation and create a chemical space map considering various similarity measures simultaneously, we report a new approach of applying reaction informatics tools to map and analyze drug pairs, namely the differential reaction fingerprint (DRFP)[21] and the Transformer-based RXNMapper model,[22–24] respectively **(Figure 1)**. These tools were initially designed to analyze chemical reactions. However, they can also be applied to processes that do not obey Lavoisier's principle, the conservation of mass, such as the alchemical transmutation of lead into gold.[25,26] Here, we apply them to transmutations between pairs of molecules selected for their similarity according to various molecular fingerprints as similarity measures, an approach related to the recent development of transformer models for drug optimization.[27,28]

We start by using DRFP, which encodes chemical reactions by storing the symmetric difference of two sets containing the circular molecular n-grams generated from the molecules of the molecular pair as a binary fingerprint,[21] to represent the chemical space of drug pairs as a TMAP (tree-map).[29] A TMAP lays out the minimum spanning tree of the nearest neighbor graphs according to a selected similarity measure, here DRFP, and represents a remarkably efficient dimensionality reduction method for high-dimensional datasets. The DRFP TMAP visualization provides a global similarity perspective across drug pairs combining the selected similarity measures. We then use RXNMapper,[22] a model trained on one million reactions documented in the USPTO dataset[30] to pair corresponding atoms between reactants and products in a chemical reaction, to identify the structural relationship between drugs. The confidence score of this

transformer appears not to correlate with any of the molecular similarity measures used. It allows us to distinguish drug pairs related by feasible chemical processes, such as matched molecular pairs corresponding to substituent exchanges,[31,32] from those related by more esoteric, alchemical transmutations including scaffold-hopping changes.[33,34] We demonstrate this approach with the example of FDA-approved drugs as a diversity set, as well as for a series of EGFR inhibitors and polymyxin B analogs as two high similarity sets chosen among small molecule drugs and peptide macrocyclic drugs, respectively.
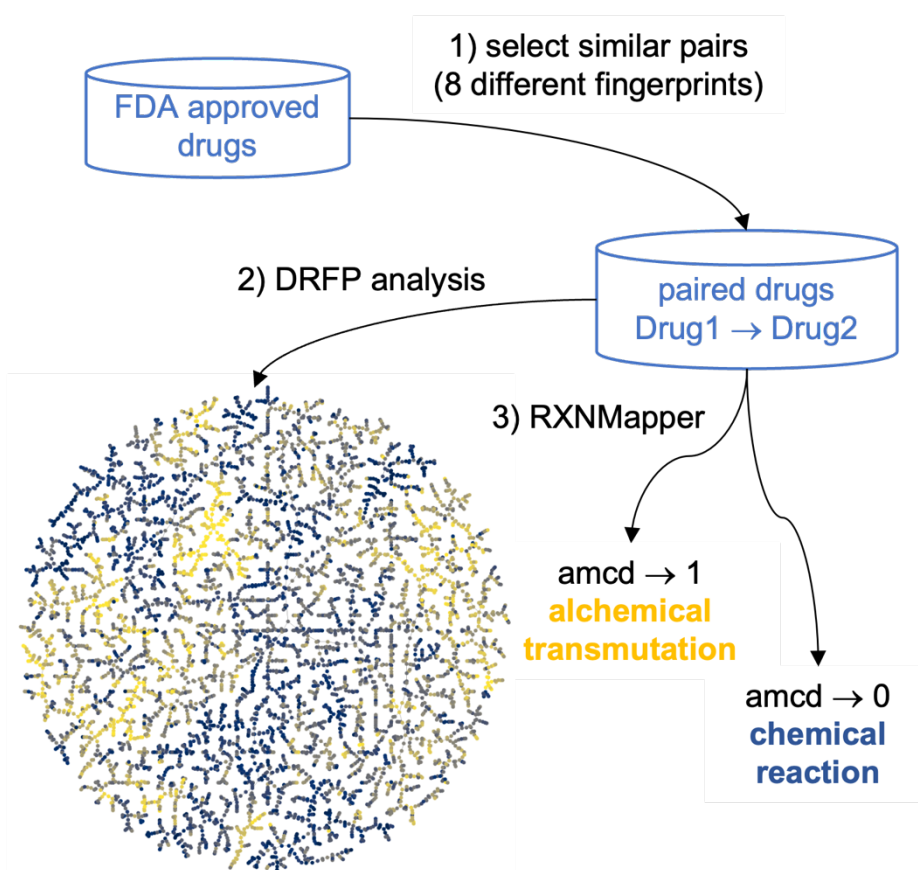

Figure 1. Principle of alchemical analysis of molecular sets at the example of FDA approved drugs. 1) Drugs pairs passing a similarity threshold according to eight different molecular fingerprints are selected. 2) The set of selected pairs is mapped in a TMAP computed using the differential reaction fingerprint (DRFP), color coded by the RXNmapper confidence distance (amcd). 3) the amcd distinguishes pairs of drugs related by a possible reaction (amcd → 0) from those related by an alchemical transmutation (amcd → 1).

Methods

Datasets

The set of FDA-approved drugs was downloaded from ZINC15,[35,36] the SMILES were canonicalized and kekulized and duplicates were removed to obtain a set of 1,213 unique chemical structures. For the EGFR set, all compounds binding to the tyrosine kinase erbB1 with a molecular weight <700 and an annotated IC_{50} value were downloaded from ChEMBL-31.[37] After SMILES canonicalization and kekulization, duplicates were removed and the 1,500 molecules with the highest ECFP4 Tanimoto similarity to afatinib were selected for the final set. The polymyxin B similarity set was downloaded from ChEMBL-31 by selecting compounds above the 55% ChEMBL similarity threshold with annotated MIC values. The SMILES were canonicalized and kekulized, and duplicates were removed resulting in a final set of 274 structures.

Molecular fingerprints and similarity calculations

Chemical structures were encoded as eight different fingerprints, namely extended connectivity fingerprints ECFP4 and ECFP6,[38,39] the MinHashed Fingerprint MHFP6,[40] the RDKit Atom-Pair Fingerprint (AP),[41] the Macromolecule Extended Fingerprint (MXFP),[42] the MinHashed Atom-Pair fingerprint MAP4,[43] the Molecular ACCess System keys (MACCS),[44] and Molecular Quantum Numbers (MQNs).[45] ECFP4, ECFP6, AP, MACCS and MQN were calculated using the implementation in the RDKit package (2022.3.4. , https://www.rdkit.org). ECFPs were calculated as 2048-bit vectors. MHFP6 and MAP4 were calculated as 2048-bit vectors using the code described in https://github.com/reymond-group/mhfp and https://github.com/reymond-group/map4. MXFP was calculated using a new open-source version available at https://github.com/reymond-group/mxfp_python. The differential reaction fingerprint (DRFP)[21] was calculated as 2048-bit vectors using the code available at https://github.com/reymond-group/drfp.

Pairwise distances for every possible molecular pair were calculated and stored as a matrix for each fingerprint. Distances were calculated as Jaccard distances (d_J) for ECFP4, ECFP6, MHFP6, AP, MAP4 and MACCS keys, and as Taxicab distances (d_T) for MXFP and MQNs, with values min-max standardized. We selected similar pairs by applying the following distance threshold: $d_J < 0.6$ for ECFP4, ECFP6, MHFP6, $d_J < 0.5$ for AP, $d_J < 0.2$ for MACCS, $d_J < 0.8$ for MAP4, $d_T < 0.1$ for MXFP and $d_T < 0.05$ for MQN (Taxicab distances after rescaling) for the FDA set and $d_J < 0.2$ for ECFP4, ECFP6, MHFP6, AP, $d_J < 0.0125$ for MACCS, $d_J < 0.3$ for MAP4, $d_T < 0.1$ for MXFP and $d_T < 0.05$ for MQN for the EGFR and PMB sets.

Additionally, the ranking of molecular pairs for every compound and fingerprint was calculated, resulting in 1,213 ranked lists of 1,213 pairs each for the FDA set, 1,500 ranked lists of 1,500 ranked pairs for the EGFR set and 274 ranked lists of 274 pairs for the polymyxin B similarity set for each fingerprint.

Violin plots to display the distribution of distances for every fingerprint and heatmaps to visualize correlations between fingerprints were generated using the seaborn (0.11.2) package. The pairwise distance distributions were balanced out by calculating the ranking of molecular pairs for every compound, resulting in 1,213 ranked lists of 1,213 pairs each for the FDA set, 1,500 ranked lists of 1,500 ranked pairs for the EGFR set and 274 ranked lists of 274 pairs for the polymyxin B similarity set.

Reaction informatics

A reaction SMILES in the form "SMILES1>>SMILES2" (forward reaction) as well as "SMILES2>>SMILES1" (backward reaction) was generated for every selected molecular pair. The forward reaction SMILES was generated to always have the molecule with the lower heavy atom count as a reactant and the molecule with the higher heavy atom count as a product. The reaction SMILES for each drug pair was then encoded using DRFP.[21] The 20 nearest neighbors (NNs) in the

DRFP feature space were extracted and the minimum spanning tree layout calculated using the TMAP package.[29] The resulting layout was displayed interactively using Faerun.[46] In addition, the atom-mapping and the corresponding atom-mapping confidence scores were computed for each drug pair reaction SMILES using the published model described in the rxnmapper[22] GitHub repository https://github.com/rxn4chemistry/rxnmapper.

Results and Discussion

Datasets and selection of drug pairs

To test our reaction informatics approach to map drug space, we selected 1,213 FDA-approved drugs as a representative high diversity set. As examples of a more focused series, we accessed the ChEMBL database[37] and retrieved 1,500 analogs of the small molecule drug afatinib, a kinase inhibitor blocking the endothelial growth factor receptor (EGFR) and used to treat non-small cell lung carcinoma (NSCLC),[47] as well as 274 analogs of polymyxin B (PMB), an FDA-approved macrocyclic peptide natural product considered as a last resort antibiotic against multidrug-resistant bacteria.[48]

To represent molecular similarities, we considered three types of molecular fingerprints. First, we selected the classical Morgan fingerprint,[38] also called extended connectivity fingerprint (ECFP),[39] which is a binary fingerprint encoding the presence of specific atom-centered circular substructures up to a diameter of four (ECFP4) and six (ECFP6) bonds, as well as our recently reported MinHashed fingerprint MHFP6,[40] which similarly encodes circular substructures up to a diameter of six bonds using shingling and MinHashing to compress information.[49] These circular substructure fingerprints are particularly efficient in virtual screening benchmarks[40,50] and off-target prediction tasks.[51,52] Second, we considered three pharmacophore fingerprints encoding the relative positions of atoms in a molecule and representing molecular shape, namely the RDKit atom-pair fingerprint AP,[41] our recently reported macromolecule extended atom-pair fingerprint MXFP,[42] and

the MinHashed Atom-pair fingerprint up to a diameter of four bonds MAP4.[43] Finally, we also

included two composition fingerprints, namely MACCS keys[44] and molecular quantum numbers

(MQN),[45] which encode the presence and number of features present in a molecule.

To identify relevant pairs in each of our three drug sets (FDA, EGFR and PMB), we

computed all pairwise distances in each fingerprint as either Jaccard distance d_J (ECFP4, ECFP6,

MHFP6, AP, MAP4, MACCS keys) or Taxicab distance d_T (MXFP, MQN). For all fingerprints,

distance zero indicates highest similarity. For each molecule in each set, we then selected the NN

for each of the eight fingerprints, as well as any molecule appearing in at least seven of the eight

lists of top-20 nearest neighbors. In addition, we selected all drug pairs having a certain similarity in

each fingerprint by applying a maximum Jaccard distance (d_J) threshold (see Methods for details).

This selection corresponded to 6,406 (0.87 %) of the 735,078 possible drug pairs in the FDA

set, 8,932 (0.79 %) of the 1,124,250 possible drug pairs in the EGFR set, and 8,464 (22.63 %) of the

37,401 possible drug pairs in the PMB set. Each drug was represented in the selected pairs between

1 and 193 times in the FDA approved set, between 1 and 870 times in the EGFR set, and between 4

and 1,031 times in the PMB set (**Figure S1**). Compared to the exhaustive list of drug pairs, the

selected drug pairs were enriched in high similarity pairs with lower values of Jaccard distance (d_J).

They spanned the entire similarity range in each fingerprint, reflecting the fact that the different

fingerprints captured different similarity features (**Figure 2a/3a/4a**). Distances were correlated

between ECFP4, ECFP6, MHFP6, MAP4, which all encode circular substructures around atoms (r^2

~ 0.8, **Figure 2b/3b/4b**). AP and MACCS, which both encode atomic features, were weakly

correlated with each other and to a lesser extent with circular fingerprints (r^2 ~ 0.5). Finally, MQN

and MXFP distances were partly correlated with each other (r^2 ~ 0.5) but not with any other

fingerprints, probably because both fingerprints are size-dependent and count similar features in

molecules.

DRFP chemical space maps

To gain a closer insight into the pairwise relationships among the selected drug pairs, we represented each pair in the form of a reaction SMILES considering the conversion of one drug into the other. Form the reaction SMILES, we then computed the differential reaction fingerprint (DRFP),[21] which encodes the circular substructures that occur only in either the reactant or the product. To represent the DRFP chemical space illustrating the similarities between different drug pairs, we then computed a tree-map (TMAP) providing an overview of drug pairs in each of the three datasets, using various color codes to visualize pair properties (**Figure 2c/3c/4c**). The TMAP of DRFP similarities organized pairs by structural types, often series of close analogs of a reference drug. Furthermore, in the FDA-approved drug set, different compound families such as amino acids, steroids, β-lactams, catecholamines, benzodiazepines or prostaglandins appeared in different regions of the map. This was visible upon close inspection of the interactive TMAPs and is illustrated here for the FDA drug set with the color FCsp^3 (**Figure 2c**).

Interactive browsing of the TMAPs made it very easy to inspect drug pairs with specific properties. For example, with the EGFR set, color-coding by activity differences pointed to the few similar drug pairs representing activity cliffs (**Figure 3c**). Inspection of TMAPs was also key to identifying interesting pairs from the point of view of their transformations, as discussed below.

Atom mapping

To estimate whether paired drugs were interconvertible by a feasible chemical reaction or required a more esoteric transmutation, we subjected the drug pair reaction SMILES to the Transformer-based RXNMapper model,[22] which returns an atom-to-atom comparison illustrating the structural relationships within pairs, as well as an atom-mapping confidence score. Atom-mapping confidence scores were determined for the forward and backward reactions and converted to atom-mapping confidence distances (amcd), defined here as one minus the confidence score. In most cases the amcd values were similar for forward and backward reactions, however since the difference was

sometimes substantial (**Figure S2**), we used the mean amcd of forward and backward reactions for our analysis. The mean amcd value spanned the entire range between low and high distance (last entry, **Figure 2a/3a/4a**) except for the PMB set, which mainly contains high confidence distances as the structures are too big for the model to map with high confidence. Further, the amcd was not correlated with any of the selected molecular similarities (last entry, **Figure 2b/3b/4b**).

Low amcd values indicated drug pairs related by a simple and usually feasible chemical transformation, usually a functional group change or addition as those found in matched molecular pairs,[31,32] illustrated in the FDA set for the hydroxylation of L-tyrosine to L-DOPA (**Figure 2d**), and in the EGFR set for a Suzuki coupling resulting in a large activity change (**Figure 3d**). In the case of the PMB set, low amcd values indicated pairs related by single amino acid exchange often potentially corresponding to a reaction, for example mutation of a glycine to a phenylalanine residue corresponding formally to an α-alkylation of glycine with benzyl bromide (**Figure S6**).

On the other hand, high amcd values indicated alchemical transmutations that cannot be realized easily, such as scaffold-hopping changes.[33,34] Note that the RXNMapper assigned corresponding atoms mostly in a correct manner even for pairs giving high amcd values. For example, tetrabenazine is paired with hydrocodone by seven of the eight molecule fingerprints used for pairing. The transformation features an exotic double-ring formation accompanied by a reshuffling of the 23 atoms (**Figure 2e**). A similarly exotic alchemical change relates afatinib with osimertinib, an analog matched by all eight fingerprints used for pairing (**Figure 2f**). In the EGFR set, a double linker modification preserving activity relates CHEMBL469997 to CHEMBL181275, whereby the benzyl ether linker is obtained by combining an oxygen atom of the sulfone with a methylene group of the aminobutanol second linker group (**Figure 3e**). In another scaffold hopping change between CHEMBL469997 and CHEMBL181275, an aniline substituent is incorporated into the adjacent bicyclic system to form a condensed tricyclic heteroaromatic group, resulting in an interesting activity increase (**Figure 3f**).

In the case of the PMB set, many pairs were generally related by high amcd values, probably because the changes corresponded to multiple amino acid exchanges, which cannot be realized on the complete molecules since each sequence analog requires a separate synthesis. Interestingly, one of the high amcd changes corresponds to a simple exchange of four aromatic aldehyde imines attached to the four diaminobutanoic acid residues, a reaction which would seem to be feasible (**Figure 4d**). This imine exchange is however accompanied by a mutation of a leucine residue to a phenylalanine.

Taken together, the analysis of the TMAP of similar drug pairs guided by DRFP similarity and amcd values allowed a rapid insight into multiple interesting comparisons between molecules in each of the three sets analyzed. Further examples of interesting pairs in the FDA approved set are provided in the Supporting information (**Figure S7**).

Conclusion

In summary, we have shown that borrowing tools from reaction informatics provides an opportunity to map multiple similarity relationships between molecules simultaneously and gain insights into interesting drug pairs that are otherwise difficult to identify. Specifically, we used DRFP to map the chemical space of multiple drug pairs selected as being similar according to eight different molecular fingerprints simultaneously in the form of TMAPs. We then used RXNMapper to visualize the structural changes between drugs and identify pairs of drugs related by feasible chemical transformation from pairs related by alchemical changes corresponding to multiple and complex structural rearrangements. These tools should generally be applicable to analyze drug sets from multiple angles in the context of drug discovery.

Code availability

The source codes and datasets used for this study are available at https://github.com/reymond-group/alchemical_pairs.
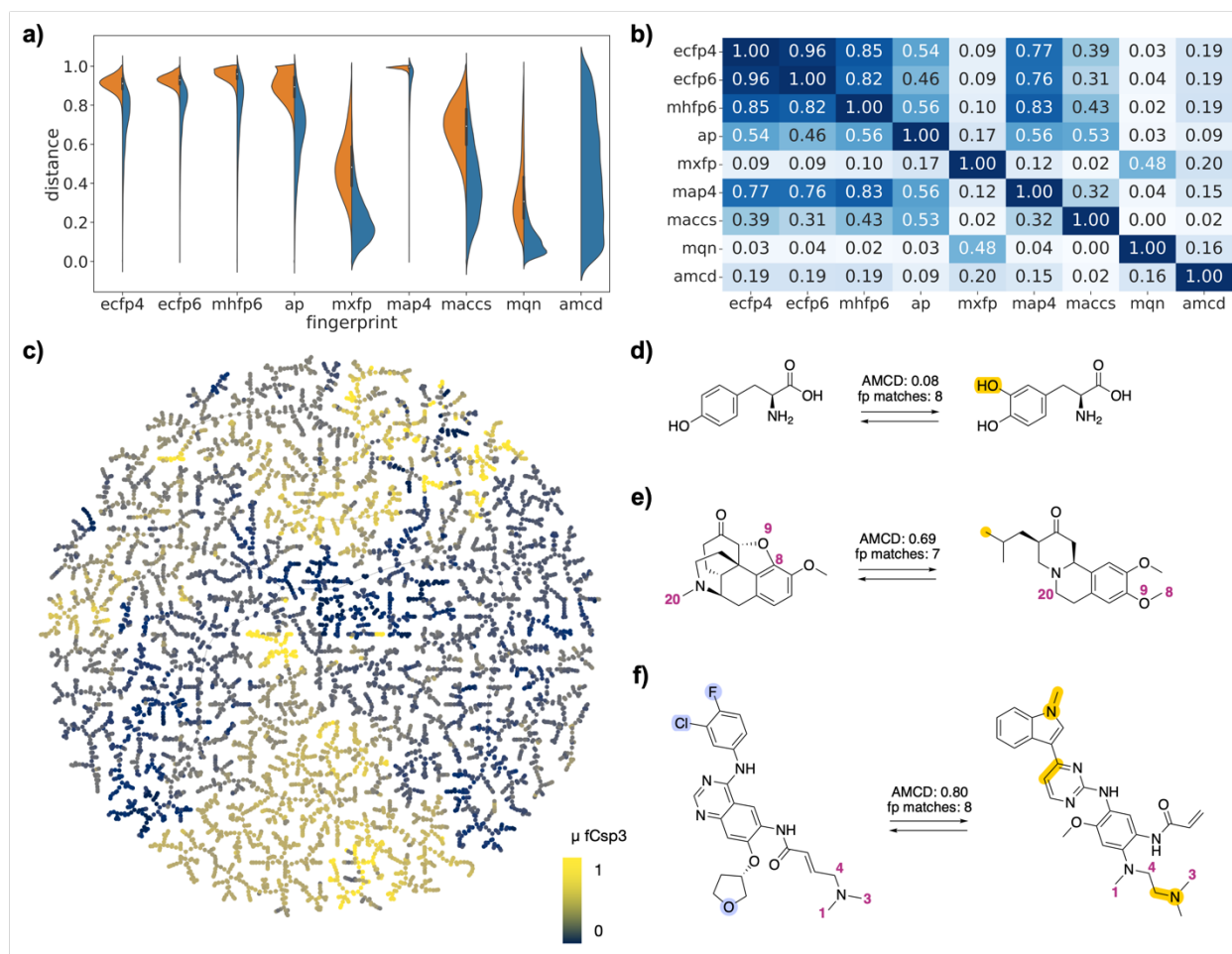
Acknowledgements

Figure 2. FDA-approved drugs as drug pairs. (**a**) Violin plot of d_J values in each of the fingerprints for all pairs (left, orange) or for selected pairs (right, blue), and for atom mapping confidence distance (amcd) of selected pairs (blue, last entry). (**b**) Heat map of correlation coefficients r^2 between d_J values of different fingerprints, and between d_J values and amcd, calculated across all selected pairs. (**c**) TMAP of DRFP similarities for selected drug pairs. Each point is a different drug pair, color-coded by the fraction of sp^3 atoms (Fsp^3). See supporting information and https://tm.gdb.tools/map4/DRFP_FDA/ for additional color codes and for the interactive version of the map. (**d**) Atom-mapped drug pair L-tyrosine and L-DOPA related by a hydroxylation reaction. (**e**) Atom-mapped drug pair tetrabenazine and hydrocodone related by an alchemical double cyclization. (**f**) Atom-mapped drug pair afatinib and osimertinib related by a series of substituent and ring system changes. Atoms highlighted in blue are lost during the forward reaction, while atoms highlighted in yellow are gained. Interesting atom rearrangements as predicted by the RXNMapper are highlighted with their respective atom-mapping number. The full atom-mapping can be found in **Figure S3**.
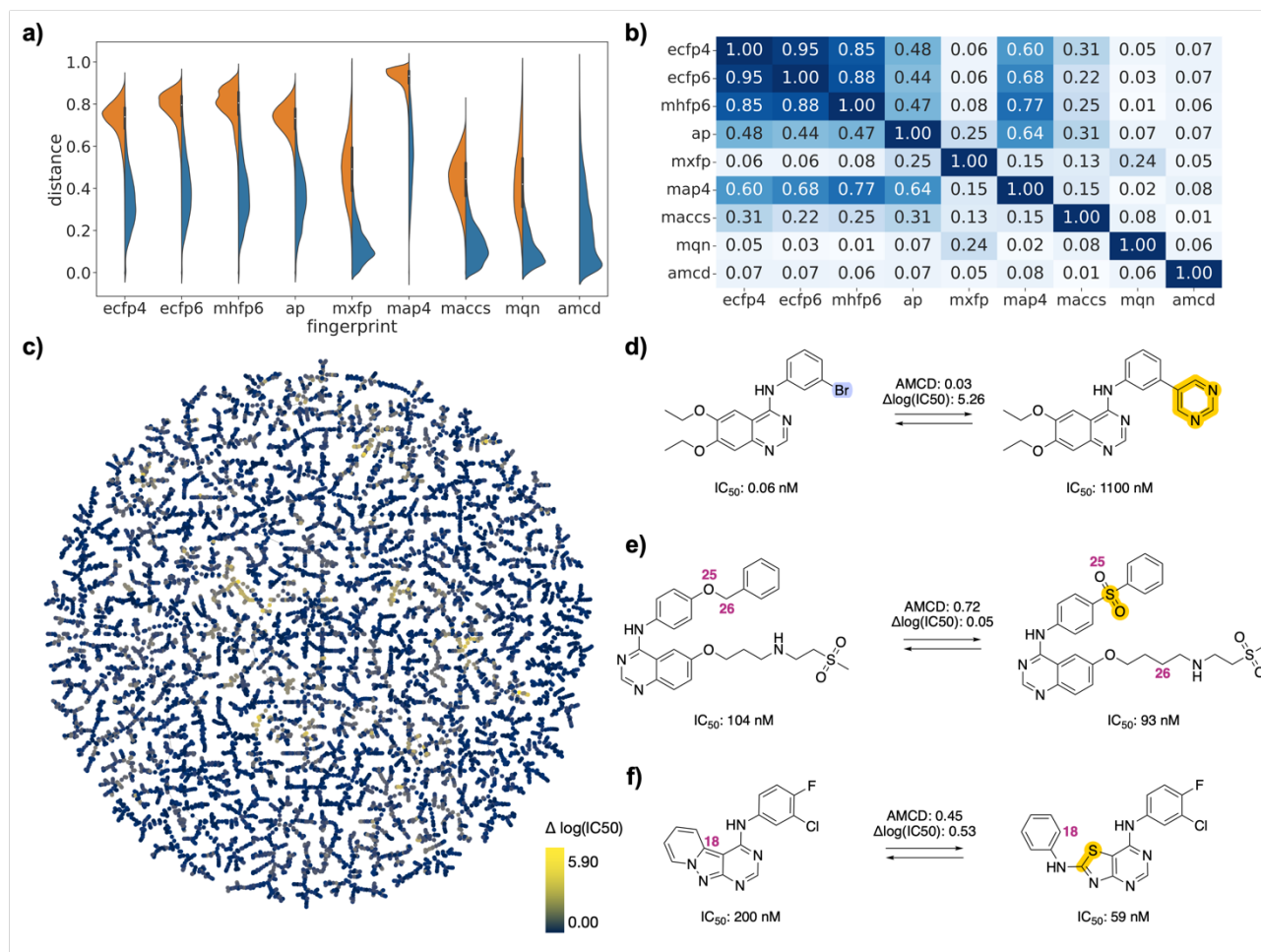
Figure 3. EGFR inhibitor drug pairs. (**a**) Violin plot of d_J values in each of the fingerprints for all pairs (left, orange) or for selected pairs (right, blue), and for atom mapping confidence distance (amcd) of selected pairs (blue, last entry). (**b**) Heat map of correlation coefficients r^2 between d_J values of different fingerprints, and between d_J values and amcd, calculated across all selected pairs. (**c**) TMAP of activity differences. Each point is a different drug pair, color-coded by the activity difference. See supporting information and https://tm.gdb.tools/map4/DRFP_EGFR/ for additional color codes and for the interactive version of the map. (**d**) Atom-mapped drug pair CHEMBL35820 and CHEMBL126974 related by a Suzuki coupling resulting in an activity cliff. (**e**) Atom-mapped drug pair CHEMBL460732 and CHEMBL14952 related by an alchemical double linker exchange preserving activity (**f**) Atom-mapped drug pair CHEMBL469997 and CHEMBL181275 related by an alchemical scaffold hopping preserving activity. Atoms highlighted in blue are lost during the forward reaction, while atoms highlighted in yellow are gained. Interesting atom rearrangements as predicted by the RXNMapper are highlighted with their respective atom-mapping number. The full atom-mapping can be found in **Figure S4**.
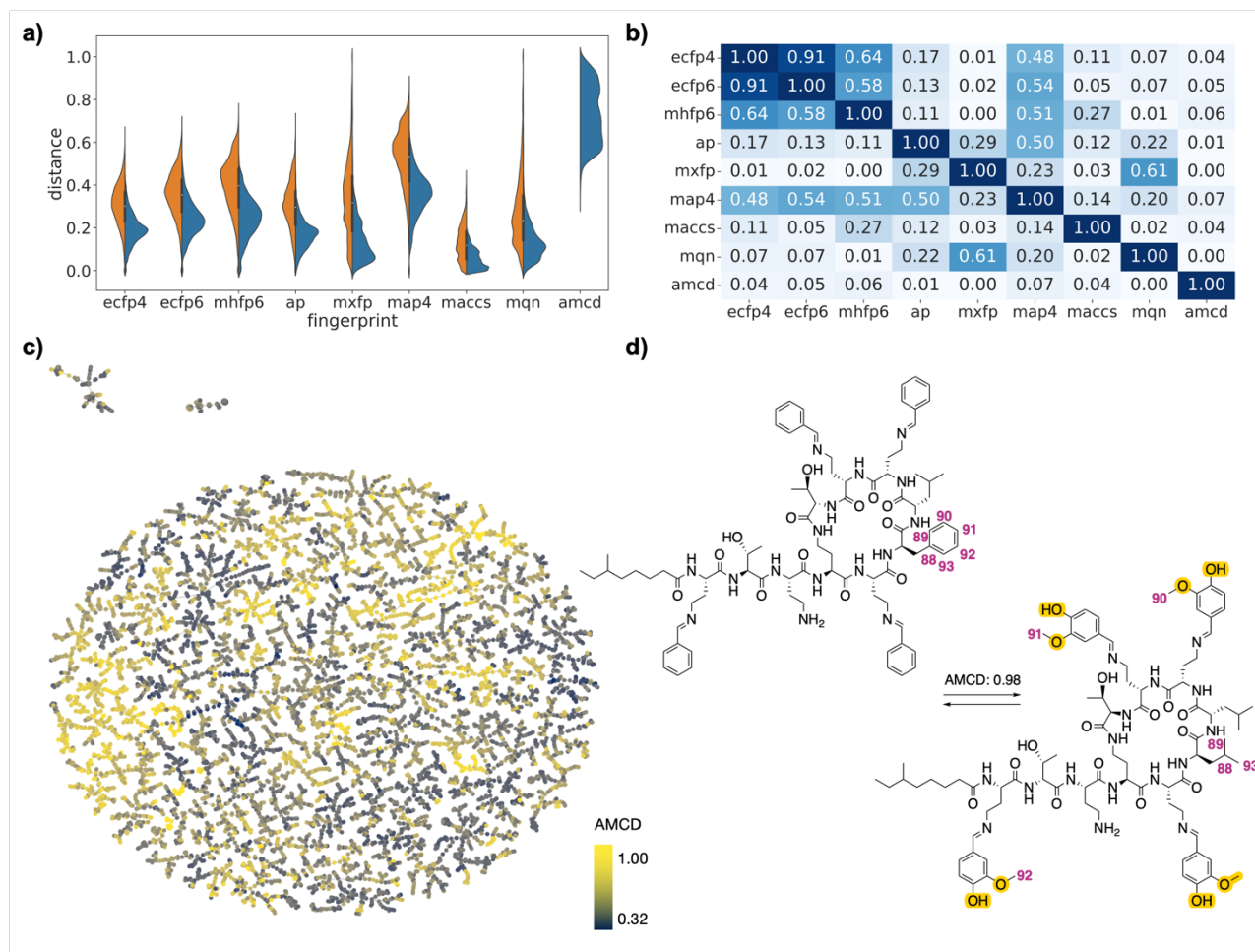
Figure 4. PMB analogs drug pairs. (**a**) Violin plot of d_J values in each of the fingerprints for all pairs (left, orange) or for selected pairs (right, blue), and for atom mapping confidence distance (amcd) of selected pairs (blue, last entry). (**b**) Heat map of correlation coefficients r^2 between d_J values of different fingerprints, and between d_J values and amcd, calculated across all selected pairs. (**c**) TMAP of amcd values. Each point is a different drug pair, color-coded by the amcd value. See supporting information and https://tm.gdb.tools/map4/DRFP_PMB/ for additional color codes and for the interactive version of the map. (**d**) Atom-mapped drug pair CHEMBL1090265 and CHEMBL2372545 related by an imine exchange and a leucine→phenylalanine mutation. Atoms highlighted in blue are lost during the forward reaction, while atoms highlighted in yellow are gained. Interesting atom rearrangements as predicted by the RXNMapper are highlighted with their respective atom-mapping number. The full atom-mapping can be found in **Figure S5**.

References

(1)   Oprea, T. I.; Gottfries, J. Chemography: The Art of Navigating in Chemical Space. *J Comb Chem* **2001**, *3* (2), 157–166.

(2)   Schuffenhauer, A.; Ertl, P.; Roggo, S.; Wetzel, S.; Koch, M. A.; Waldmann, H. The Scaffold Tree – Visualization of the Scaffold Universe by Hierarchical Scaffold Classification. *J Chem Inf Model* **2007**, *47* (1), 47–58. https://doi.org/10.1021/ci600338x.

(3)   Ivanenkov, Y. A.; Savchuk, N. P.; Ekins, S.; Balakin, K. V. Computational Mapping Tools for Drug Discovery. *Drug Discov. Today* **2009**, *14* (15–16), 767–775. http://dx.doi.org/10.1016/j.drudis.2009.05.016.

(4)   Wassermann, A. M.; Wawer, M.; Bajorath, J. Activity Landscape Representations for Structure–Activity Relationship Analysis. *J. Med. Chem.* **2010**, *53* (23), 8209–8223. https://doi.org/10.1021/jm100933w.

(5)   Sharma, S.; Arya, A.; Cruz, R.; Cleaves II, H. J. Automated Exploration of Prebiotic Chemical Reaction Space: Progress and Perspectives. *Life* **2021**, *11* (11), 1140. https://doi.org/10.3390/life11111140.

(6)   Andronov, M.; Fedorov, M. V.; Sosnin, S. Exploring Chemical Reaction Space with Reaction Difference Fingerprints and Parametric T-SNE. *ACS Omega* **2021**, *6* (45), 30743–30751. https://doi.org/10.1021/acsomega.1c04778.

(7)   Capecchi, A.; Reymond, J.-L. Classifying Natural Products from Plants, Fungi or Bacteria Using the COCONUT Database and Machine Learning. *J. Cheminformatics* **2021**, *13* (1), 82. https://doi.org/10.1186/s13321-021-00559-3.

(8)   Vriza, A.; Sovago, I.; Widdowson, D.; Kurlin, V.; A. Wood, P.; S. Dyer, M. Molecular Set Transformer: Attending to the Co-Crystals in the Cambridge Structural Database. *Digit. Discov.* **2022**, *1* (6), 834–850. https://doi.org/10.1039/D2DD00068G.

(9)   Medina-Franco, J. L.; Sánchez-Cruz, N.; López-López, E.; Díaz-Eufracio, B. I. Progress on Open Chemoinformatic Tools for Expanding and Exploring the Chemical Space. *J. Comput. Aided Mol. Des.* **2022**, *36* (5), 341–354. https://doi.org/10.1007/s10822-021-00399-1.

(10)   Humer, C.; Heberle, H.; Montanari, F.; Wolf, T.; Huber, F.; Henderson, R.; Heinrich, J.; Streit, M. ChemInformatics Model Explorer (CIME): Exploratory Analysis of Chemical Model Explanations. *J. Cheminformatics* **2022**, *14* (1), 21. https://doi.org/10.1186/s13321-022-00600-z.

(11)   Beckers, M.; Fechner, N.; Stiefl, N. 25 Years of Small-Molecule Optimization at Novartis: A Retrospective Analysis of Chemical Series Evolution. *J. Chem. Inf. Model.* **2022**, *62* (23), 6002–6021. https://doi.org/10.1021/acs.jcim.2c00785.

(12)   Zabolotna, Y.; Bonachera, F.; Horvath, D.; Lin, A.; Marcou, G.; Klimchuk, O.; Varnek, A. Chemspace Atlas: Multiscale Chemography of Ultralarge Libraries for Drug Discovery. *J. Chem. Inf. Model.* **2022**, *62* (18), 4537–4548. https://doi.org/10.1021/acs.jcim.2c00509.

(13)   Cihan Sorkun, M.; Mullaj, D.; Koelman, J. M. V. A.; Er, S. ChemPlot, a Python Library for Chemical Space Visualization**. *Chemistry–Methods* **2022**, *2* (7), e202200005. https://doi.org/10.1002/cmtd.202200005.

(14) Han, M.; Liu, S.; Zhang, D.; Zhang, R.; Liu, D.; Xing, H.; Sun, D.; Gong, L.; Cai, P.; Tu, W.; Chen, J.; Hu, Q.-N. AddictedChem: A Data-Driven Integrated Platform for New Psychoactive Substance Identification. *Molecules* **2022**, *27* (12), 3931. https://doi.org/10.3390/molecules27123931.

(15) Moshawih, S.; Hadikhani, P.; Fatima, A.; Goh, H. P.; Kifli, N.; Kotra, V.; Goh, K. W.; Ming, L. C. Comparative Analysis of an Anthraquinone and Chalcone Derivatives-Based Virtual Combinatorial Library. A Cheminformatics "Proof-of-Concept" Study. *J. Mol. Graph. Model.* **2022**, *117*, 108307. https://doi.org/10.1016/j.jmgm.2022.108307.

(16) Nicholls, A.; McGaughey, G. B.; Sheridan, R. P.; Good, A. C.; Warren, G.; Mathieu, M.; Muchmore, S. W.; Brown, S. P.; Grant, J. A.; Haigh, J. A.; Nevins, N.; Jain, A. N.; Kelley, B. Molecular Shape and Medicinal Chemistry: A Perspective. *J Med Chem* **2010**, *53* (10), 3862–3886. https://doi.org/10.1021/jm900818s.

(17) Maggiora, G.; Vogt, M.; Stumpfe, D.; Bajorath, J. Molecular Similarity in Medicinal Chemistry. *J. Med. Chem.* **2014**, *57* (8), 3186–3204. https://doi.org/10.1021/jm401411z.

(18) Willett, P. Similarity-Based Virtual Screening Using 2D Fingerprints. *Drug Discov. Today* **2006**, *11* (23–24), 1046–1053. https://doi.org/10.1016/j.drudis.2006.10.005.

(19) Awale, M.; Reymond, J. L. Similarity Mapplet: Interactive Visualization of the Directory of Useful Decoys and ChEMBL in High Dimensional Chemical Spaces. *J Chem Inf Model* **2015**, *55* (8), 1509–1516. https://doi.org/10.1021/acs.jcim.5b00182.

(20) J. Jesús Naveja; Medina-Franco, J. L. ChemMaps: Towards an Approach for Visualizing the Chemical Space Based on Adaptive Satellite Compounds, 2017. https://doi.org/10.5256/F1000RESEARCH.12095.D171632.

(21) Probst, D.; Schwaller, P.; Reymond, J.-L. Reaction Classification and Yield Prediction Using the Differential Reaction Fingerprint DRFP. *Digit. Discov.* **2022**, *1* (2), 91–97. https://doi.org/10.1039/D1DD00006C.

(22) Schwaller, P.; Hoover, B.; Reymond, J.-L.; Strobelt, H.; Laino, T. Extraction of Organic Chemistry Grammar from Unsupervised Learning of Chemical Reactions. *Sci. Adv.* **2021**, *7* (15), eabe4166. https://doi.org/10.1126/sciadv.abe4166.

(23) Devlin, J.; Chang, M.-W.; Lee, K.; Toutanova, K. BERT: Pre-Training of Deep Bidirectional Transformers for Language Understanding. arXiv May 24, 2019. https://doi.org/10.48550/arXiv.1810.04805.

(24) Lan, Z.; Chen, M.; Goodman, S.; Gimpel, K.; Sharma, P.; Soricut, R. ALBERT: A Lite BERT for Self-Supervised Learning of Language Representations. arXiv February 8, 2020. https://doi.org/10.48550/arXiv.1909.11942.

(25) Ball, P. Alchemical Culture and Poetry in Early Modern England. *Interdiscip. Sci. Rev.* **2006**, *31* (1), 77–92. https://doi.org/10.1179/030801806X84246.

(26) Wentrup, C. Chemistry, Medicine, and Gold-Making: Tycho Brahe, Helwig Dieterich, Otto Tachenius, and Johann Glauber. *ChemPlusChem* **2023**, *88* (1), e202200289. https://doi.org/10.1002/cplu.202200289.

(27) He, J.; You, H.; Sandström, E.; Nittinger, E.; Bjerrum, E. J.; Tyrchan, C.; Czechtizky, W.; Engkvist, O. Molecular Optimization by Capturing Chemist's Intuition Using Deep Neural

Networks. *J. Cheminformatics* **2021**, *13* (1), 26. https://doi.org/10.1186/s13321-021-00497-0.

(28) He, J.; Nittinger, E.; Tyrchan, C.; Czechtizky, W.; Patronov, A.; Bjerrum, E. J.; Engkvist, O. Transformer-Based Molecular Optimization beyond Matched Molecular Pairs. *J. Cheminformatics* **2022**, *14* (1), 18. https://doi.org/10.1186/s13321-022-00599-3.

(29) Probst, D.; Reymond, J.-L. Visualization of Very Large High-Dimensional Data Sets as Minimum Spanning Trees. *J. Cheminformatics* **2020**, *12* (1), 12. https://doi.org/10.1186/s13321-020-0416-x.

(30) Lowe, Daniel. Chemical Reactions from US Patents (1976-Sep2016). *figshare. dataset.* **2017**. https://doi.org/10.6084/m9.figshare.5104873.v1.

(31) Kramer, C.; Fuchs, J. E.; Whitebread, S.; Gedeck, P.; Liedl, K. R. Matched Molecular Pair Analysis: Significance and the Impact of Experimental Uncertainty. *J. Med. Chem.* **2014**, *57* (9), 3786–3802. https://doi.org/10.1021/jm500317a.

(32) Awale, M.; Riniker, S.; Kramer, C. Matched Molecular Series Analysis for ADME Property Prediction. *J. Chem. Inf. Model.* **2020**, *60* (6), 2903–2914. https://doi.org/10.1021/acs.jcim.0c00269.

(33) Schneider, G.; Neidhart, W.; Giller, T.; Schmid, G. "Scaffold-Hopping" by Topological Pharmacophore Search: A Contribution to Virtual Screening. *Angew Chem Int Ed Engl* **1999**, 38 (19), 2894–2896.

(34) Böhm, H.-J.; Flohr, A.; Stahl, M. Scaffold Hopping. *Drug Discov. Today Technol.* **2004**, *1* (3), 217–224. https://doi.org/10.1016/j.ddtec.2004.10.009.

(35) Sterling, T.; Irwin, J. J. ZINC 15 – Ligand Discovery for Everyone. *J. Chem. Inf. Model.* **2015**, *55* (11), 2324–2337. https://doi.org/10.1021/acs.jcim.5b00559.

(36) Irwin, J. J.; Tang, K. G.; Young, J.; Dandarchuluun, C.; Wong, B. R.; Khurelbaatar, M.; Moroz, Y. S.; Mayfield, J.; Sayle, R. A. ZINC20—A Free Ultralarge-Scale Chemical Database for Ligand Discovery. *J. Chem. Inf. Model.* **2020**. https://doi.org/10.1021/acs.jcim.0c00675.

(37) Mendez, D.; Gaulton, A.; Bento, A. P.; Chambers, J.; De Veij, M.; Félix, E.; Magariños, M. P.; Mosquera, J. F.; Mutowo, P.; Nowotka, M.; Gordillo-Marañón, M.; Hunter, F.; Junco, L.; Mugumbate, G.; Rodriguez-Lopez, M.; Atkinson, F.; Bosc, N.; Radoux, C. J.; Segura-Cabrera, A.; Hersey, A.; Leach, A. R. ChEMBL: Towards Direct Deposition of Bioassay Data. *Nucleic Acids Res.* **2019**, *47* (D1), D930–D940. https://doi.org/10.1093/nar/gky1075.

(38) Morgan, H. L. The Generation of a Unique Machine Description for Chemical Structures-A Technique Developed at Chemical Abstracts Service. *J Chem Doc* **1965**, *5* (2), 107–113. https://doi.org/10.1021/c160017a018.

(39) Rogers, D.; Hahn, M. Extended-Connectivity Fingerprints. *J. Chem. Inf. Model.* **2010**, *50* (5), 742–754. https://doi.org/10.1021/ci100050t.

(40) Probst, D.; Reymond, J.-L. A Probabilistic Molecular Fingerprint for Big Data Settings. *J. Cheminformatics* **2018**, *10* (1), 66. https://doi.org/10.1186/s13321-018-0321-8.

(41) Carhart, R. E.; Smith, D. H.; Venkataraghavan, R. Atom Pairs as Molecular Features in Structure-Activity Studies: Definition and Applications. *J. Chem. Inf. Comput. Sci.* **1985**, *25* (2), 64–73. https://doi.org/10.1021/ci00046a002.

(42) Capecchi, A.; Awale, M.; Probst, D.; Reymond, J. PubChem and ChEMBL beyond Lipinski. *Mol. Inform.* **2019**, *38* (5), 1900016. https://doi.org/10.1002/minf.201900016.

(43) Capecchi, A.; Probst, D.; Reymond, J.-L. One Molecular Fingerprint to Rule Them All: Drugs, Biomolecules, and the Metabolome. *J. Cheminformatics* **2020**, *12* (1), 43. https://doi.org/10.1186/s13321-020-00445-4.

(44) Durant, J. L.; Leland, B. A.; Henry, D. R.; Nourse, J. G. Reoptimization of MDL Keys for Use in Drug Discovery. *J. Chem. Inf. Comput. Sci.* **2002**, *42* (6), 1273–1280. https://doi.org/10.1021/ci010132r.

(45) Nguyen, K. T.; Blum, L. C.; van Deursen, R.; Reymond, J.-L. Classification of Organic Molecules by Molecular Quantum Numbers. *ChemMedChem* **2009**, *4* (11), 1803–1805. https://doi.org/10.1002/cmdc.200900317.

(46) Probst, D.; Reymond, J.-L. FUn: A Framework for Interactive Visualizations of Large, High-Dimensional Datasets on the Web. *Bioinformatics* **2018**, *34* (8), 1433–1435. https://doi.org/10.1093/bioinformatics/btx760.

(47) Yang, Z.; Hackshaw, A.; Feng, Q.; Fu, X.; Zhang, Y.; Mao, C.; Tang, J. Comparison of Gefitinib, Erlotinib and Afatinib in Non-Small Cell Lung Cancer: A Meta-Analysis. *Int. J. Cancer* **2017**, *140* (12), 2805–2819. https://doi.org/10.1002/ijc.30691.

(48) Nordmann, P.; Poirel, L. Plasmid-Mediated Colistin Resistance: An Additional Antibiotic Resistance Menace. *Clin Microbiol Infect* **2016**, *22* (5), 398–400. https://doi.org/10.1016/j.cmi.2016.03.009.

(49) Damashek, M. Gauging Similarity with N-Grams: Language-Independent Categorization of Text. *Science* **1995**, *267* (5199), 843–848. https://doi.org/10.1126/science.267.5199.843.

(50) Riniker, S.; Landrum, G. A. Open-Source Platform to Benchmark Fingerprints for Ligand-Based Virtual Screening. *J Cheminf* **2013**, *5* (1), 26. https://doi.org/10.1186/1758-2946-5-26.

(51) Awale, M.; Reymond, J. L. Web-Based Tools for Polypharmacology Prediction. *Methods Mol Biol* **2019**, *1888*, 255–272. https://doi.org/10.1007/978-1-4939-8891-4_15.

(52) Awale, M.; Reymond, J.-L. Polypharmacology Browser PPB2: Target Prediction Combining Nearest Neighbors with Machine Learning. *J Chem Inf Model* **2019**, *59* (1), 10–17. https://doi.org/10.1021/acs.jcim.8b00524.

Supplementary Information for: Alchemical Analysis of FDA Approved Drugs

Markus Orsi,[a] Daniel Probst,[b] Philippe Schwaller[b] and Jean-Louis Reymond[a]*

a) *Department of Chemistry, Biochemistry and Pharmaceutical Sciences, University of Bern,*

Freiestrasse 3, 3012 Bern, Switzerland, [b)]*Ecole Polytechnique Fédérale de Lausanne, 1015*

Lausanne, Switzerland

e-mail: *jean-louis.reymond@unibe.ch*

Table of Contents

1. Supplementary figures
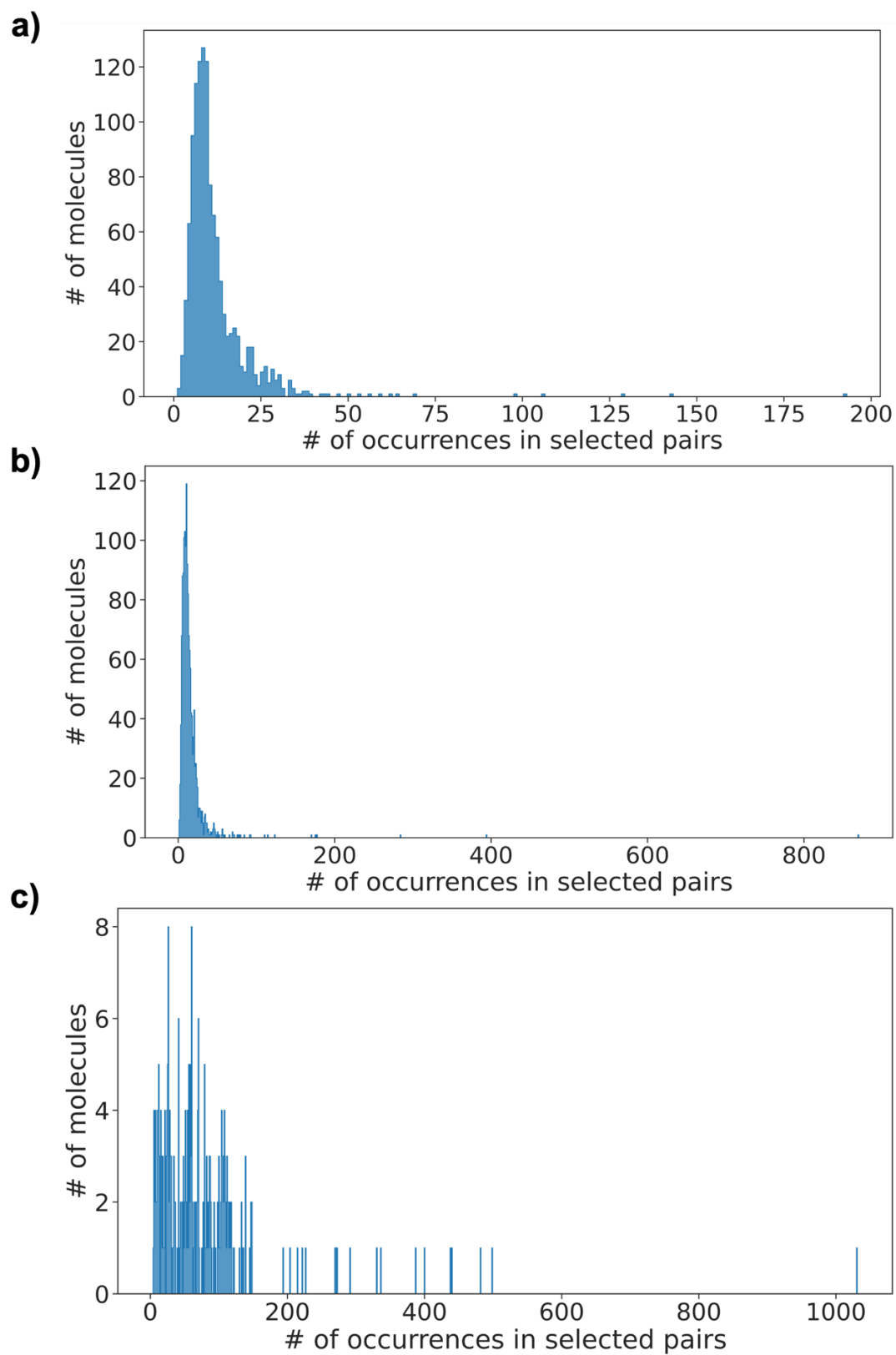
Figure S1. Count of molecules by number of occurrences in selected pairs for the a) FDA, b) EGFR and c) PMB set. In all sets, most of the molecules appear sporadically in the selected pairs. Only a limited number of compounds appears more often.
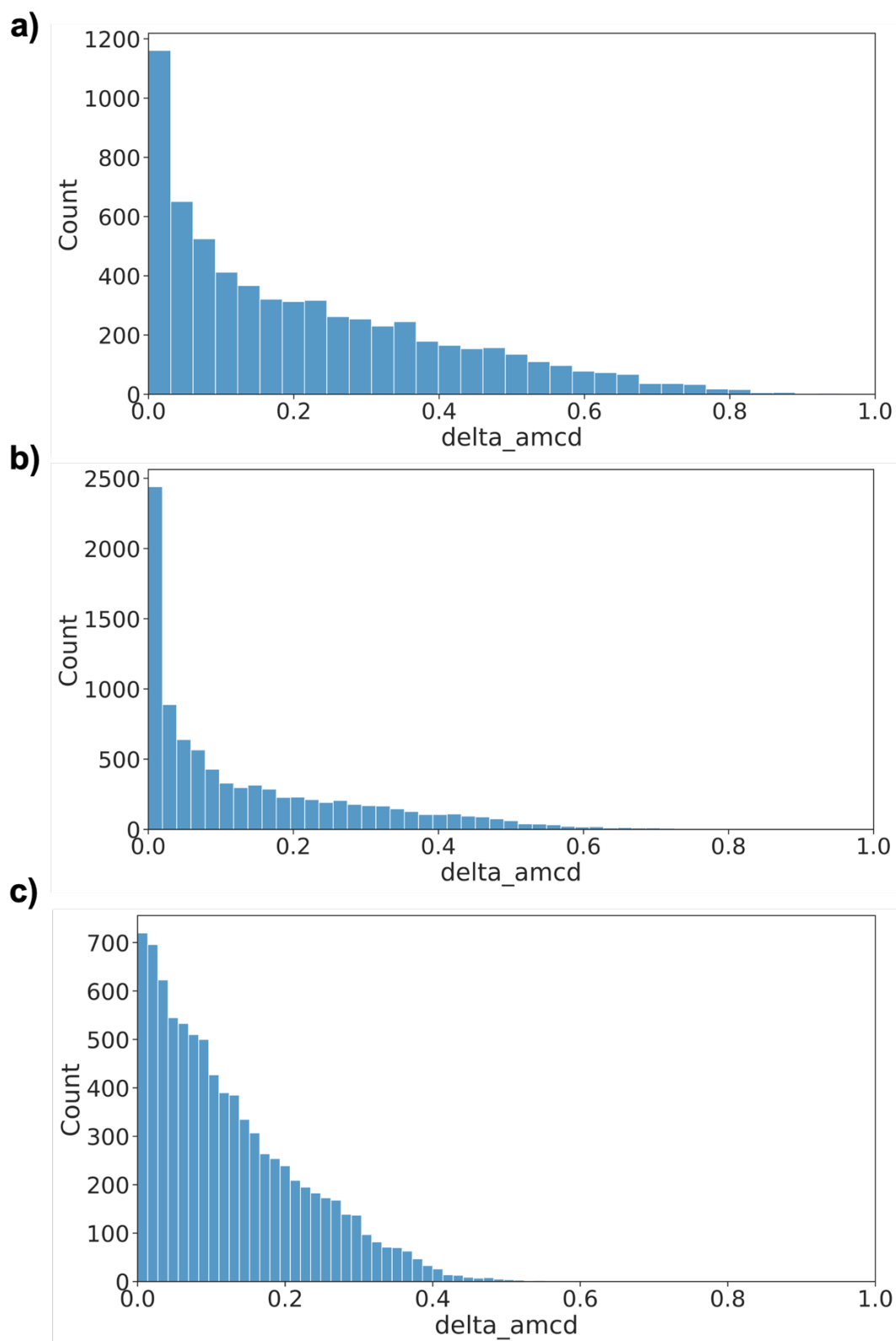
Figure S2. Count of molecular pairs by difference in atom-mapping confidence score between the forward and backward reactions in selected pairs for the a) FDA, b) EGFR and c) PMB set.
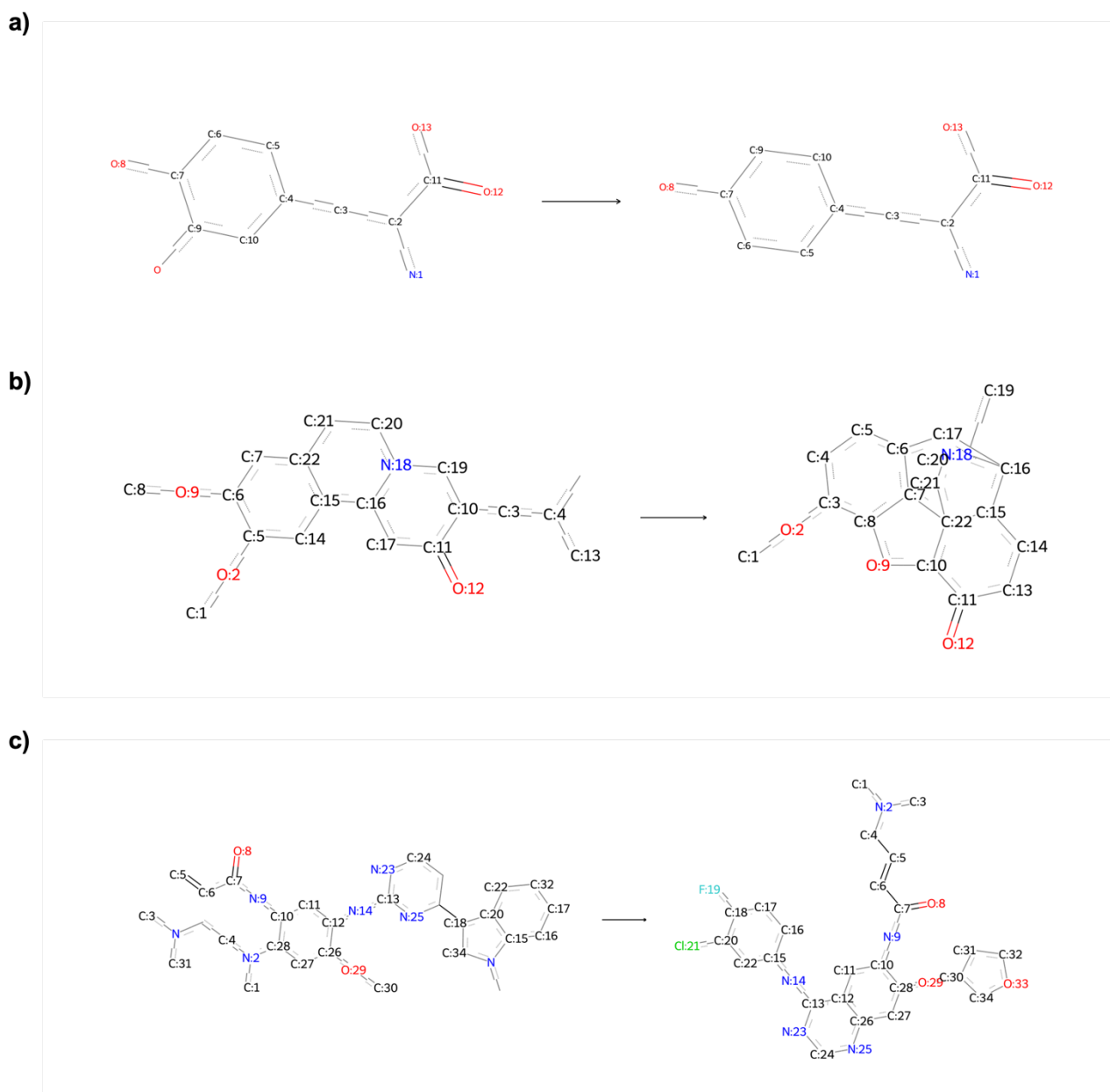
Figure S3. Full atom mapping of the examples selected from the FDA set. The shown atom-mapping is the one of the backwards reactions.
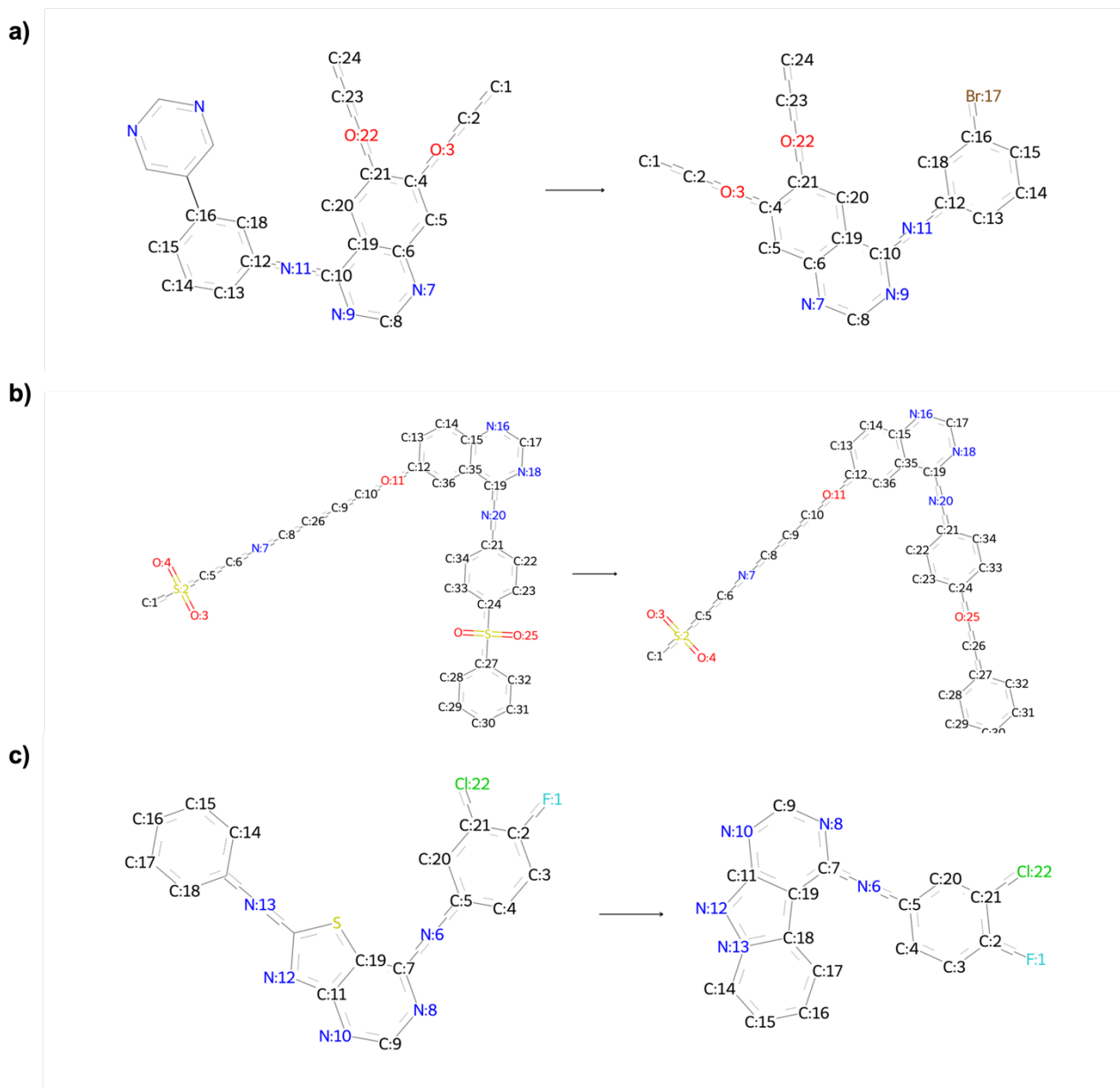
Figure S4. Full atom mapping of the examples selected from the EGFR set. The shown atom-mapping is the one of the backwards reactions.
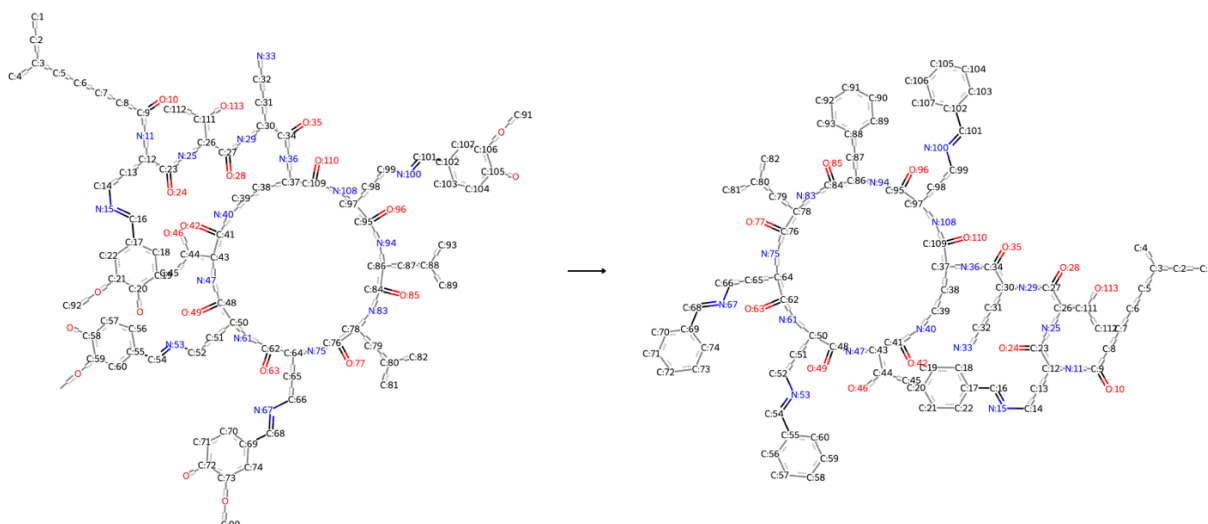
Figure S5. Full atom mapping of the example selected from the PMB set. The shown atom-mapping is the one of the backwards reaction.
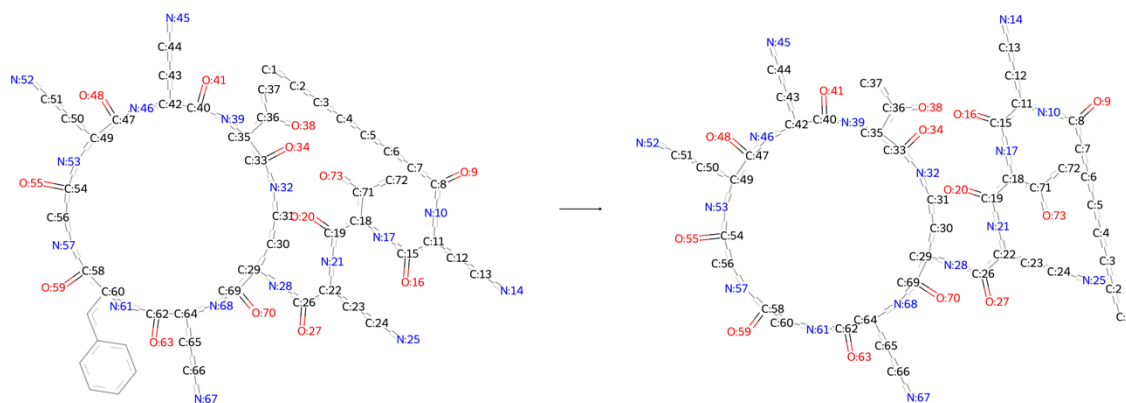

Figure S6: Full atom-mapping of mutation of a glycine to a phenylalanine residue (amcd: 0.32), corresponding to a feasible α-alkylation reaction of glycine with benzyl bromide.
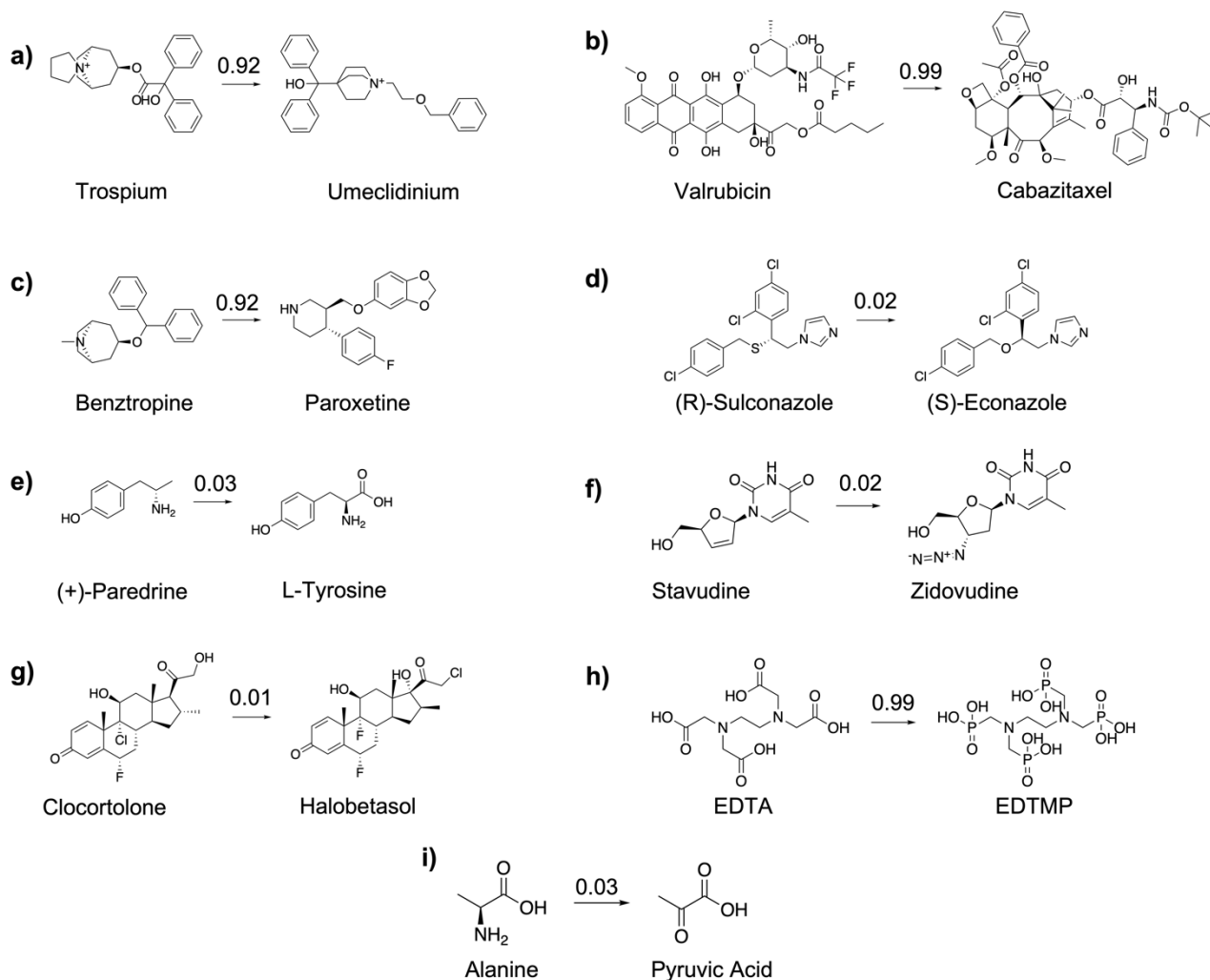
Figure S7: Additional interesting pairs selected from the drug pairs in the FDA-approved subset and the determined atom-mapping confidence distance of the reaction. a) Trospium and Umeclidinium, two anticholinergic drugs acting on the muscarinic receptor. The structures contain common elements, such as the diphenylmethanol and tropane-like moieties, which are completely rearranged between the two structures. b) Valrubicin and Cabazitaxel, two anticancer drugs acting on topoisomerase II and tubulin stabilization respectively. Although the two compounds act on different targets, these targets are part of the same pathway and their inhibition leads to cell death. c) Benztropine and Paroxetine, two unrelated drugs acting on serotonin uptake inhibition. d) (R)-Sulconazole and (S)-Econazole, two imidazole antifungals differing from each other by a single atom mutation from S to O. e) (+)-Paredrine and L-Tyrosine, two closely related structures separated by an alchemical condensation of a carboxylic acid to a methyl and stereo-inversion. f) Stavudine and Zidovudine, two HIV reverse transcriptase inhibitors separated by an azidation. g) Clocortolone and Halobetasol, two steroid drugs used for the treatment of inflammatory and itching skin diseases. h) EDTA and EDTMP, both highly related chelating agents. i) Alanine and Pyruvic Acid, two highly related compounds separated by a N to =O mutation.